An Examination of Subsonic Airfoils For The Development of Drone Wings

Gopalakrishnan Dharmaraj Ms
Dept of Aerospace Engineering
University Of Hertfordshire, Uk.

Abstract- *The development of drone technology has exploded in recent years, despite the fact that the field of aeronautics already has a significant amount of technology. The human species is now in a position where it can more easily travel by air, carry out monitoring and surveillance, and even have product delivery that are more cheaply priced and open the door for urban development. This is in comparison to prior times.*

The purpose of this study is to examine a variety of airfoils by making use of the principles of computational fluid dynamics in order to determine which of these airfoils is the most effective for the construction of aircraft wings, which are an essential component.

The extruded airfoil curve is created by using the airfoil coordinates from the online tool known as airfoil tools. Next, the flow over the extruded airfoil is simulated using CFD techniques with the necessary parameters to check the attitude of the air and visualize boundary layer separation and vortices using contours.

I. INTRODUCTION

The E176 and the SA 7038 are the two airfoils that I have opted to concentrate on for this study. I made use of a web-based application to generate the coordinates in the form of a text file so that I could import them with relative ease.

After that, each coordinate is included into the formation of an airfoil.

After then, the drag, lift, and other forces that are experienced by each extruded airfoil are measured in order to determine which one will be the greatest candidate for further development into a 3D wing model. The simulation has taken into account a wide variety of elements, including density, angle of attack, boundary condition, and vortex, to name just a few of them.

II. OBJECTIVES

This research will hopefully result in the development of an acceptable airfoil for the wing of a drone. After that, you should carry out a computational simulation in order to determine its external influences. After selecting the airfoils that produce the least amount of drag while still producing substantial forces, the best airfoils are used to generate the wing model. This model is then improved further by making precise alterations to its design and measurement in order to select the optimal wing design.

III. METHODOLOGY

For this task, two different types of airfoil coordinates must be converted into a 3D model using Solid Works. A 2D design is first created in line with the estimated value, and the surface is then produced using an extrusion. The modelled item is then saved in a format that the CFD simulation programme, such as Starccm+, would be able to read. To create a perfect mesh, the imported 3D curve coordinates should next be subdivided in the proper way, including naming the extruded airfoils and defining the domain's border where they are placed for analysis.

Next, the meshing process is carried out as a form of preprocessing by selecting the appropriate Meshing Technique (Method- quadrilaterals and Type of Mesh - Mapped Mesh.) Following mesh generation, the domain and airfoil should be combined using a BOOLEAN OPERATION SUCH AS SUBTRACTION.

The physics of the geometry, such as continuity and the energy equation, should be taken into account as a third process. Additionally, based on the requirements and conditions, the sort of boundary condition that should be provided can be selected by picking velocity and pressure values of 18 m/s and 101325 p.a (atmospheric pressure), respectively. The setup must finally be started and computed over a larger number of iterations for the simulation's computation to eventually settle on the modelled nose cone shape.

The very last step, but certainly not the least, is the post-processing phase, which entails visualizing plots, vectors, contours, and other criteria based on demands or even curiosity. Before we go too further into the study, let's take a look at what an airfoil is, the different forms of it, and its nomenclature.

The term "airfoil" refers, in general, to the sectional area of a wing that is cut across.

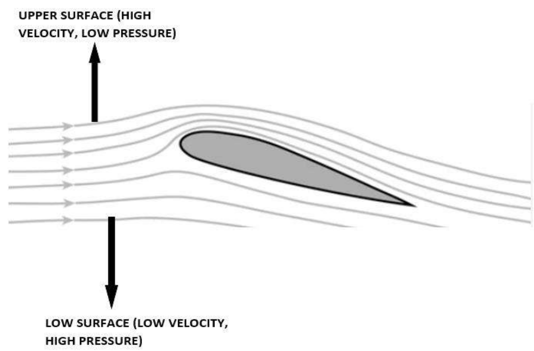

FIG 1: AIRFOIL (COURTESY: SHUTTER SHOCK)

IV. FACTORS LEADING TO HIGH LIFT

1. SHAPE.
2. VELOCITY.
3. DENSITY.
4. SURFACE AREA.
5. ANGLE OF ATTACK.

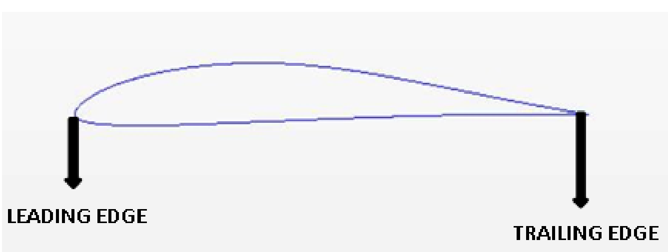

FIG 2: AIRFOIL (SA 7038)

LEADING EDGE

The portion of the airfoil that makes the first contact with the air.

TRAILING EDGE

The portion of the airfoil that makes its first contact with the air last.

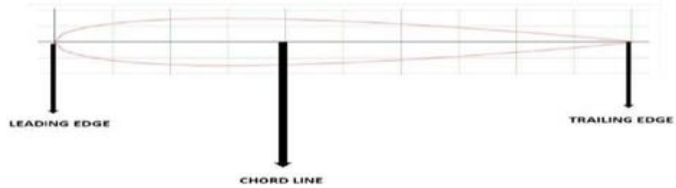

FIG 3: AIRFOIL (COURTESY: CARL PATON)

CHORD

The distance from the leading edge to the back edge.

CHORD LINE

A line that runs in a straight line from the leading edge of the airfoil to the trailing edge.

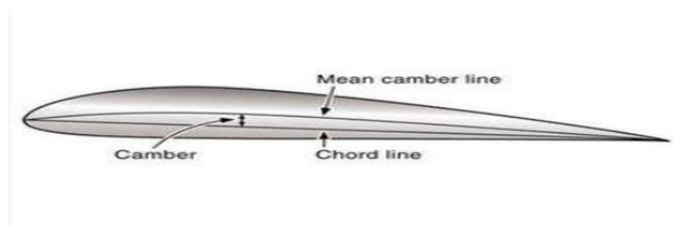

FIG 4: AIRFOIL (COURTESY: AVIATION STACK EXCHANGE)

CAMBER LINE

A line that is equidistant from the top and bottom surfaces and connects the leading edge with the trailing edge.

CAMBER

Measurement taken from the chord line back to the camber line.

ANGLE OF ATTACK

Measure of the angle formed by the chord line and the relative wind.

FIG 5: AIRFOIL (COURTESY: HOME PILOT)

STALL

A stall happens when the wings lose their ability to provide lift because the smooth airflow over them collapses and the airflow mostly separates from them. When circulation breaks out, lift drops drastically while drag rises dramatically. The stall angle for a particular wing size and shape is determined by the angle of attack.

AOA'	CL
0	4.53
2	7.3
2.5	7.8
5	9.5
10	10.9
15	9.35
20	5.29
25	5.11

TABLE 1 : COEFFICIENT LIFT VS ANGLE OF ATTACK

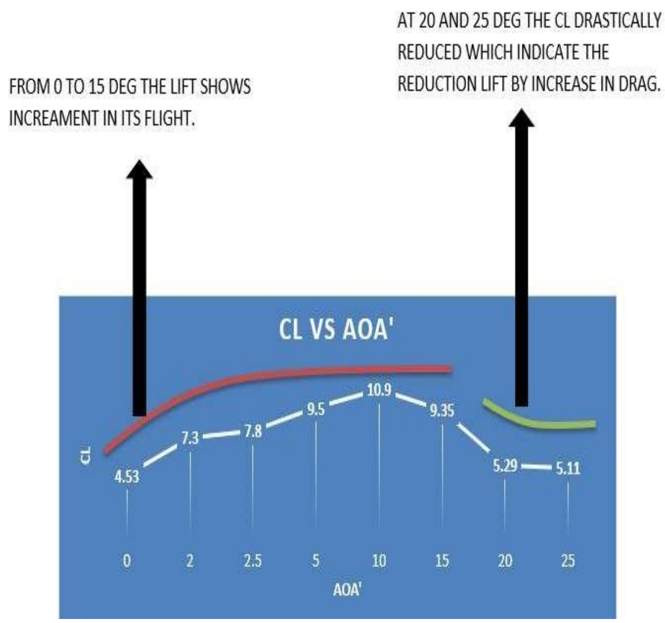

FIG 6: GRAPH OF CL VS AOA'

STALL ANGLE

The angle of attack at which the phenomena of stalling may be said to take place.

V. TYPES OF AIRFOILS

The airfoils may be divided into two distinct categories. They are,

1. **Symmetry Airfoil.**
2. **Asymmetry Airfoil.**

SYMMETRICAL

A symmetrical airfoil has parallel upper and lower surfaces that are similar in appearance. There is no difference between the chord and the camber line.

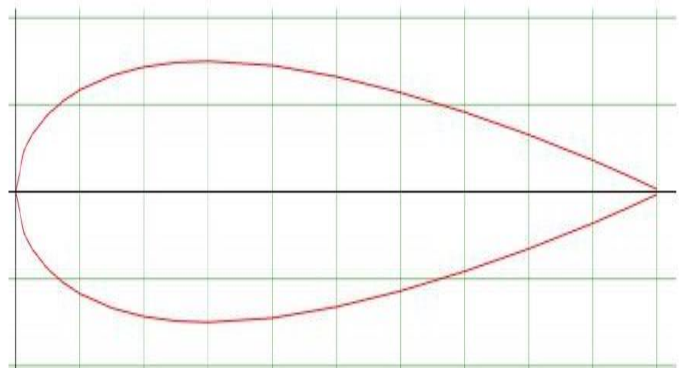

FIG 7: SYMMETRICAL AIRFOIL – NACA 0015 (COURTESY: AIRFOIL TOOLS)

ASYMMETRICAL

Both the top and bottom surfaces of the asymmetrical airfoil are distinct from one another. The chord and the camber line are distinct from one another in that they both exhibit considerable thickness.

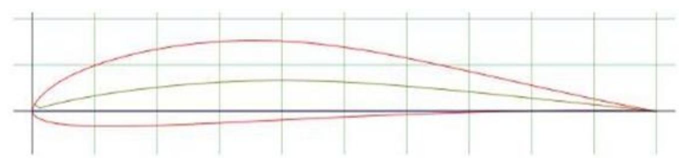

FIG 8: ASYMMETRICAL AIRFPOIL - E176 (COURTESY: AIRFOIL TOOLS)

NATIONAL ADVISORY COMMITTEE OF AERONAUTICS NOMENCLATURE.

The airfoil was categorized based on the series by the national advisory council of Aeronautics for the United States of America.

NACA 4 DIGIT SERIES

NACA 2412.

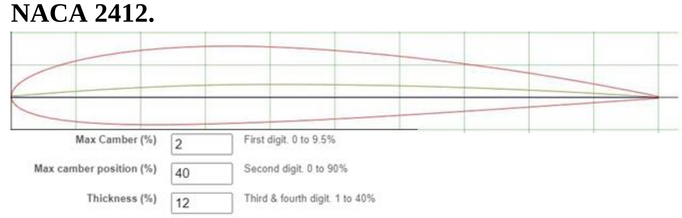

FIG 9: NACA 4 DIGIT SERIES – NACA 2412. (COURTESY: AIRFOIL TOOLS)

NACA 0018

FIG 10: NACA 0018. (COURTESY: AIRFOIL TOOLS)

NACA 5 DIGIT SERIES

NACA 23015

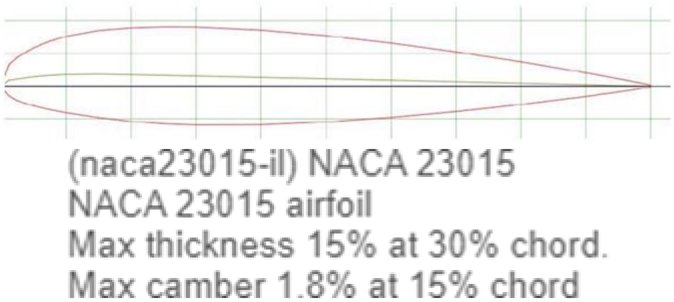

FIG 11: NACA 23015. (COURTESY: AIRFOIL TOOLS)

NACA 6 DIGIT SERIES

NACA 64(1)-212

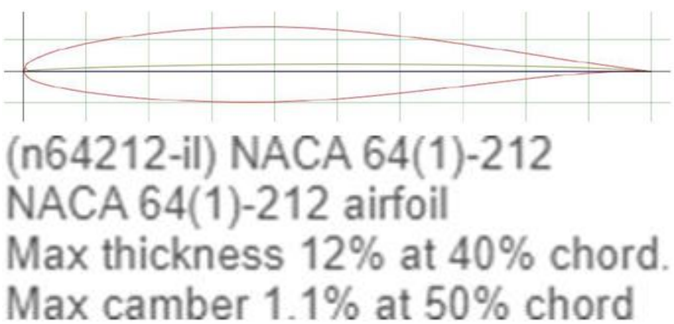

FIG 12: NACA 64(1)-212. (COURTESY: AIRFOIL TOOLS)

The design of the wing for the drone was decided upon using the theoretical understanding of airfoil, and the two airfoils that were deemed to be the best were E176 and SA 7038. As I indicated earlier in the approach, the CFD simulation was carried out in accordance with each phase, and the essential parameters—including velocity of 18 meters per second, pressure of 101325 Pascal's, and density of 1.225 kilograms per cubic meter—were selected. Within these confines, the contours of both the velocity and the pressure were shown.

VELOCITY CONTOURS

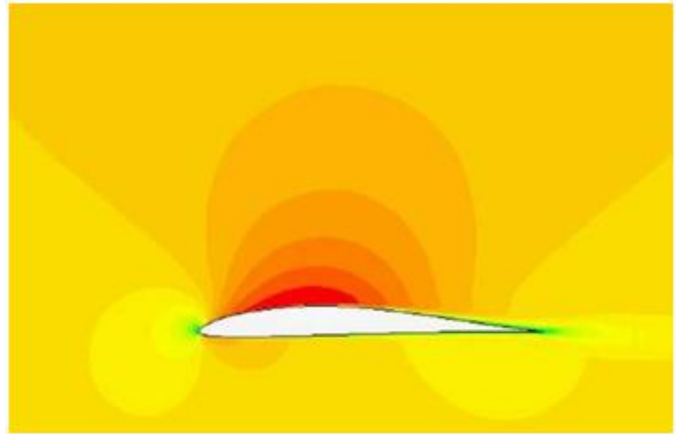

FIG 13: E176 (AOA'- 0DEG)

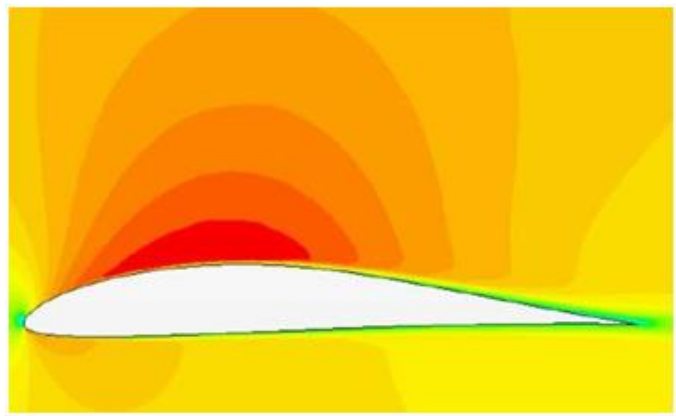

FIG 14: SA7038 (A0A' - 0DEG)

PRESSURE CONTOURS

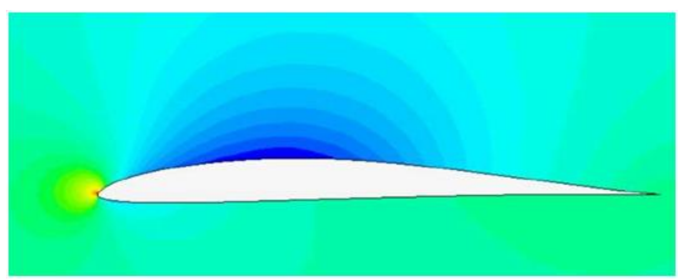

FIG 15: E176 (AOA' – 0DEG)

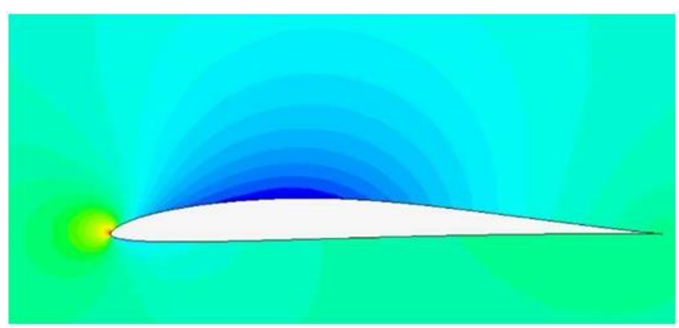

FIG 16: SA7038 (AOA' – 0DEG)

Each airfoil is simulated with the same velocity and density of 18 meters per second and1.225 Pascal's with an angle of attack of zero degrees. On the basis of the findings, i.e., the lift and drag values, the optimal airfoil is selected, and then that airfoil in particular is investigated using both a positive and a negative angle of attack while maintaining the same density and velocity as was discussed before.

LIFT AND DRAG FOR EACH AIRFOILS (E176 & SA7038)

TABLE 2: LIFT AND DRAG VALUE FOR AIRFOILS

AIRFOIL	LIFT (N)	DRAG (N)
E176	58.9251939716029	2.0044468112920932
SA7038	59.043025610215345	2.0036761249709865

The lift and drag of each airfoil is stated in the table that was just discussed, and the airfoil that has the highest lift and the lowest drag is highlighted in the table. Following this, velocity and pressure contours have been shown for each angle of attack so that the data may be seen in a more clear and concise manner.

VELOCITY CONTOUR OF SA7038

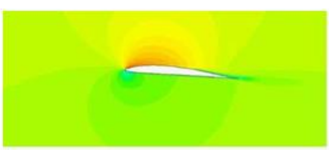

FIG 17: AIRFOIL SA7038 -5 AOA'

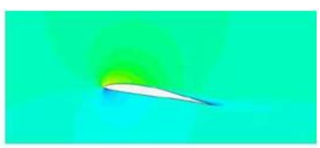

FIG 18: AIRFOIL SA7038 -10 AOA'

FIG 19: AIRFOIL SA7038 +5 AOA'

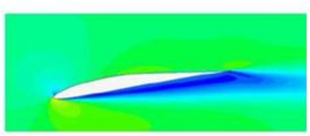

FIG 20: AIRFOIL SA7038 +10 AOA'

Even though it has the same characteristics like velocity and density at each angle of attack, the airfoil displays a varied flow pattern due to the shape of the flow.

PRESSURE CONTOUR

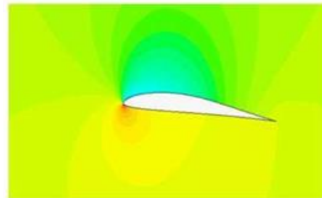

FIG 21: AIRFOIL SA7038 -5 AOA'

FIG 22: AIRFOIL SA7038 -10 AOA'

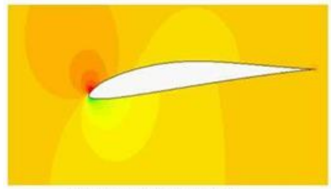

FIG 23: AIRFOIL SA7038 +5 AOA'

FIG 24: AIRFOIL SA7038 +10 AOA'

The variation in pressure that occurs as a result of a change in the angle of attack is shown quite clearly in the pressure contour that has been presented above. Depending on the circumstances, the angle of attack may either be raised or lowered; hence, the pressure can exhibit a wide range of change in both the lift and the drag forces that it encounters.

The boundary layer separation may be observed rather clearly over the object with the assistance of these contours.

BOUNDARY LAYER THEOREM

It was mentioned earlier that the body in stationary motion has a velocity of zero, which means that the velocity of the fluid particle will automatically get reduced to zero while it is remaining on the boundary of the solid body. A streamline flow with a velocity is being sent to the stationary solid body, and the fluid particle that will cling on the surface of that solid body will maintain the same velocity as the solid body. However, according to the theory, the particle will not be in a state of rest at any point in time.

Within a short amount of time, the particle of fluid flows and shows evidence of velocity gradient. Velocity gradient is the term used to describe differences in velocity in proportion to distance. After passing through the layer, the velocity will resume its free-flowing condition and return to its original value. These alterations to the velocity will only be maintained for a brief period of time inside the layer. The term "boundary layer" refers to the phenomena that takes place when there is a shift in the velocity of particles that are contained inside a thin layer. Within this boundary layer, shear stress is generated for a small amount of time; however, as soon as the velocity reaches the freestream condition, the shear stress will no longer be present and will be equal to zero.

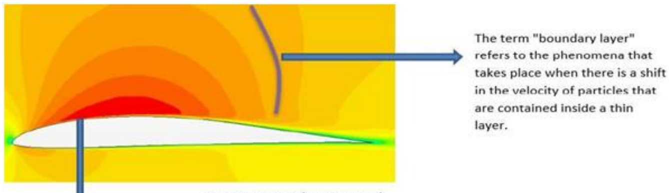

FIG 25: SA7038 (AOA' - 0DEG)

VORTEX

An area in a fluid in which the flow rotates around an axis line, which may be straight or curved, is referred to as a vortex in the field of fluid dynamics. Vortices may form in both laminar and turbulent flows. When fluids are disturbed, vortices may develop. These can be seen as smoke rings, whirlpools in the wake of a boat, and in the winds that surround a tropical cyclone, tornado, or dust devil.

In turbulent flow, vortices make up a significant portion of the flow. The idea of circulation, the distribution of velocity, and the vorticity of the flow are all used to characterize vortices. Vorticity may be thought of as the curl of the flow velocity. In the majority of vortices, the velocity of the fluid flow is highest adjacent to the axis of the vortex, and it falls in inverse proportion to the distance from the axis.

CALCULATION

In this experiment, two different airfoils were evaluated head-to-head, and the one that performed the best in terms of crucial metrics like lift and drag was selected as the winner.

LIFT

The motion of the fluid all around the item will result in the application of a force on the surface of the object. The term "lift" refers to the component of this force that exerts its action in a direction that is perpendicular to the object. The lift is calculable using a formula, and it may be expressed in terms of Newtons.

$$\mathbf{L = 0.5\ \rho\ V^2SCL}$$

SCIENTIFIC NOTATION:

1. L = LIFT.
2. ρ = DENSITY OF FLUIDS.
3. V = VELOCITY OF FLUIDS.
4. S = THE SURFACE AREA OF THE OBJECT.
5. CL = COEFFICIENT OF LIFT.

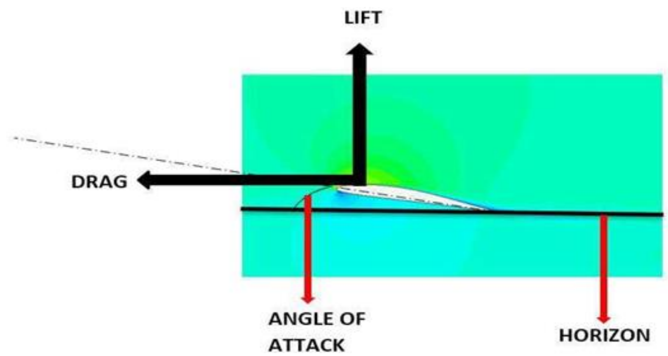

FIG 26: LIFT

DRAG

The fluid moving all around the object will exert a force on its surface. Lift is the name for a part of this force that acts perpendicular to the object. The formula for calculating the drag, which can be measured in Newtons, is

$$\mathbf{D = 0.5\ \rho\ V^2SCD}$$

SCIENTIFIC NOTATION:

1. D= DRAG.
2. ρ = DENSITY OF FLUIDS.
3. V = VELOCITY OF FLUIDS.
4. S = THE SURFACE AREA OF THE OBJECT.
5. CD = COEFFICIENT OF DRAG.

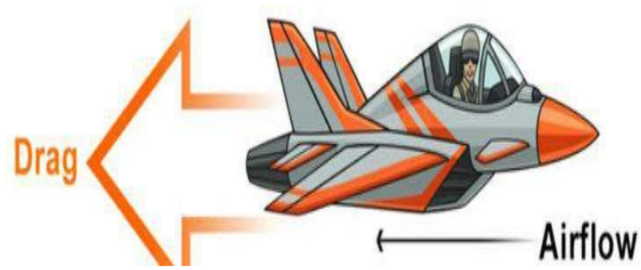

FIG 27: DRAG (COURTESY: AEROSPACE NOTES)

LIFT AND DRAG OF SA 7038

TABLE 2: LIFT AND DRAG FOR VARIOUS AOA' OF SA 7038 AIRFOIL

AOA'	LIFT	DRAG
0	59.043025610215345	2.0036761249709865
-5	164.7350727503132	2.487436033989776
-10	258.98857842384535	4.41956535628389
5	-48.19313739506608	2.4920863173871637
10	-75.46556869901828	13.993467180728464

The lift and drag values of the SA7038 airfoil have been examined in the table above with various Angles of Attack ranging from positive to negative. Here, the positive is expressed by a minus sign, and the negative by a plus sign. Therefore, it is evident that lift increases with increasing Angle of Attack from zero to plus 10, while drag increases with increasing Angle of Attack such as (+ 5 & + 10).

Curiously, the angle of attack is likewise raised, but eventually, as I previously said in Table 1, it begins to display Stall.

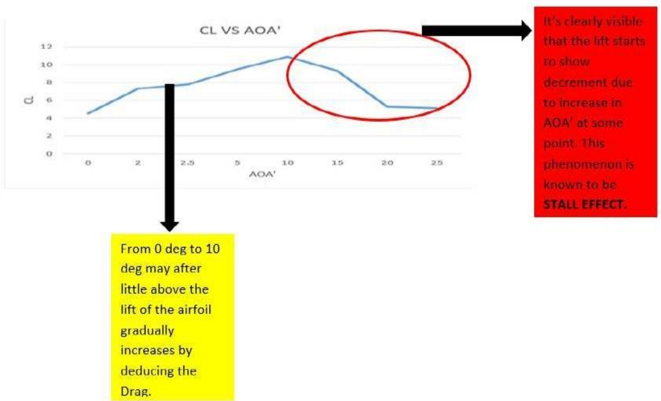

FIG 28: GRAPH OF CL VS AOA'

CALCULATION

AOA' = 0Deg,

$$L = 0.5\ \rho\ V^2 S C_L$$

$$C_L = 2L / \text{density} * \text{velocity} * \text{surface area}$$

$$C_L = 2*59.04 / 1.225 * 18 * 18 * 1$$

$$C_L = 0.2975.$$

$$D = 0.5\ \rho\ V^2 S C_D$$

$$C_D = 2D / \text{density} * \text{velocity} * \text{surface area}$$

$$C_D = 2*2.003 / 1.225 * 18 * 18 * 1$$

$$C_D = 0.01$$

VI. CONCLUSION

The outcome of this project is that out of two different airfoils, namely E176 and SA7038, the best one is picked to analyses the fluid flow over the surface and also determine the lift and drag values for both positive and negative angles of attack. At the lowest possible speed, the flow over the airfoil produces better results up to a certain angle of attack (AOA), but after that point, it begins to exhibit the stall effect, in which the lift decreases as a result of an increase in drag. It's possible that a 3D model may be used to run this simulation, which would help with comprehension of the prospective research.

REFERENCES

[1] Patel, K.S., Patel, S.B., Patel, U.B. and Ahuja, A.P., 2014. CFD Analysis of an Aerofoil. *International Journal of Engineering Research*, *3*(3), pp.154-158.

[2] Chi, X., Zhu, B., Shih, T., Addy, H. and Choo, Y., 2004. CFD analysis of the aerodynamics of a business-jet airfoil with leading-edge ice accretion. In *42nd AIAA Aerospace sciences meeting and exhibit* (p. 560).

[3] Narsipur, S., Pomeroy, B. and Selig, M., 2012, June. CFD analysis of multielement airfoils for wind turbines. In *30th AIAA applied aerodynamics conference* (p. 2781).

[4] Dash, A., 2016. CFD Analysis ofWind Turbine Airfoil at Various Angles of Attack. *IOSR J. Mech. Civ. Eng*, *13*, pp.18-24.

[5] Almheiri, Z., Aleid, R. and Dol, S.S., 2021. Design of Fixed-Wing and Multi-Copter Hybrid Drone System for Human Body Temperature Measurement during COVID-19 Pandemic. *WSEAS Transactions on Systems*, *20*, pp.31-39.